

Ion Beam Based Techniques for Mercury Cadmium Telluride Infrared Detectors

R. Pal, Vandna Mittal, R. K. Sharma, and P. K. Basu

Solid State Physics Laboratory, Delhi-110 054

ABSTRACT

The paper reviews the applications of ion beam-based techniques such as ion implantation and ion beam milling, for *HgCdTe* detector fabrication. Fabrication of large-format arrays and two-color arrays necessitate the use of dry processes. Ion irradiation causes type conversion in *HgCdTe*. The type conversion is far beyond the damage sites because of *Hg* in-diffusion to interstitial sites. The dry processes combine high anisotropy, faster etch rates, and better dimensional control, than wet etch processes, but require the damaged region to be removed.

Keywords: Infrared detectors, mercury-cadmium-telluride detectors, ion implantation, ion beam milling, detector fabrications, IR detectors, reactive ion etching, etching processes

1. INTRODUCTION

HgCdTe is a material of strategic importance for thermal imaging applications. During the initial phases of process development, wet chemical processes were predominantly employed to fabricate *HgCdTe*-based detector arrays. Futuristic and current generation thermal imagers require more reliable, high performance large format detector arrays with multicolor detection and multi-task capability packed in each pixel of the arrays¹. Fabrication of such arrays necessitated the introduction of dry processes like ion beam milling, ion implantation, reactive ion etching (RIE), high density plasma etching (HDPE) and low energy electron enhanced etching (LE4) for a number of processing steps. These dry processes facilitate:

- (a) fabrication of *n* on *p* or *p* on *n*, junctions through ion implantation, ion-beam milling (IBM) and plasma induced junction formation methods such as RIE and ECR-RIE,
- (b) milling of via holes for fabrication of high density vertically integrated photodiodes (HDVIP's) and avalanche photodiodes (APD's),
- (c) surface conversion from *n* to *n*⁺ using IBM or RIE,
- (d) mesa etching for delineation of high-density detector arrays using RIE, IBM and high-density plasma etching techniques (ECR, ICP, LE4, DRIE etc.) and
- (e) surface and/or contact cleaning using microwave/RF plasma ashing or very low-energy argon ion milling.

Although a number of dry process techniques are being successfully used in the silicon and *GaAs* industry yet their introduction in the *HgCdTe* device fabrication has been slow paced due to a number of scientific and technological difficulties². This is because the material is soft and defect prone, and its composition is sensitive to ion plasma and heating².

However, continuous efforts to solve these problems have led to the successful utilisation of some of the dry

processes in this industry as well. Agnihotri³, *et al.* reviewed the junction formation in *HgCdTe* by some of these techniques for the fabrication of photovoltaic detectors. Altaf⁴, *et al.* have reviewed the overall dry processes for *HgCdTe* infrared detectors. Present review is comprehensive study of ion beam-based techniques to evaluate all facets of these techniques from the process and device perspective, and hence, assess their relative effectiveness, merits, and suitability.

This review includes an extensive set of data for above-mentioned applications to *HgCdTe* and thus presents a holistic picture of all the scientific and technological issues involved in the utilisation of these ion beam processes. Process complexities differ depending on the application; the authors have tried to review each application.

2. ION INTERACTION WITH SOLIDS

The ion interaction, up to a certain energy density, can be successfully described as a series of binary collisions involving the impinging ion and recoiling substrate atoms, as a collision cascade⁵. Under low ion energy density, when the interaction of ion with a solid is on the surface of substrate and the ion energy is more than the binding energy of the substrate atoms, quasi-elastic collisions of ion with substrate atom leads to physical sputtering, commonly known as ion beam milling. These quasi-elastic collisions produce displacement of substrate atoms from their lattice position. Due to the energetic particle bombardment of the substrate surface, it becomes highly stressed region.

When a crystal is subjected to ionising radiation, additional vacancies and interstitials are created, in concentrations which may far exceed those produced thermally. These excess vacancies may therefore enhance the rate of diffusion, particularly at relatively low temperatures. There are two cases to consider:

- (i) the vacancy enhancement may be brought about by

- the implantation of the impurity species itself or
- (ii) the vacancies may be created by some other ionising radiation, in which case the impurity atoms may have been previously introduced either by diffusion or by implantation.

2.1 Ion Beam Milling

Ion beam milling employs ion bombardment in the energy range of 200–1500 eV, usually by Ar ions. The bombarding energy is dissipated close to the surface so that it causes atoms to be ejected from the surface. Ion beam milling technique is being implemented for various uses in small-dimension HgCdTe detector arrays. Wotherspoon⁶, Blackman⁷, *et al.* and Baker⁸, *et al.* have reported the *p* to *n* type conversion of HgCdTe using ion-milling technique. Application of ion beam milling enables fabrication of photodiodes without the need to implant any specifically donor like atoms⁹. Due to ion bombardment, Hg interstitials (Hg_i) are liberated near the surface, which diffuse into the bulk or out diffuse from the surface. According to diffusion model, diffusion of Hg is driven by a combined interstitial-vacancy mechanism. Initially, the concentration of Hg_i at the surface increases. These Hg_i diffuse into the bulk, recombine with the Hg vacancies and an *n*-type region is created. After switching off the ion source, Hg_i recombine at the *p*-*n* junction and at the surface¹⁰. The model could be justified by assuming a fast diffusion coefficient for the Hg_i (~10⁻⁶ cm²/s at 50 °C) in comparison to normal slow diffusion coefficient of Hg (~10⁻¹⁰-10⁻⁹ cm²/s at 400 °C)⁹. Investigation of ion milling by Blackman, *et al* showed that type conversion of vacancy-doped *p*-HgCdTe to *n*-HgCdTe is rate limited by the dose⁷.

Mittal¹¹, *et al.* have studied the electrical properties of *n*-HgCdTe subjected to ion beam etching by the ion beam energy 500 eV with ion beam current densities of 0.3 to 0.6 mA/cm². The excess carrier concentration after ion milling is found to be $2 \times 10^{17}/\text{cm}^3 - 2 \times 10^{18}/\text{cm}^3$. It varies with ion dose and stabilizes at around $2 \times 10^{18}/\text{cm}^3$. The change in Hg atoms (if this increase is solely due to the Hg interstitials) will be ~ 0.0003 per cent. The change in the lattice will not be much at such lower value of concentration changes. Material removal is accompanied by movement of a small concentration of group II atoms (~0.02 per cent of Hg liberated) into the lattice in the form of interstitials. The results imply that mercury interstitials diffuse very rapidly at ambient temperatures, so that subsequent Hg atoms arrive very quickly at the interface between converted and unconverted material. The phenomenon of increase in excess carrier concentration is similar to that for *p*-type material. If the material when vacancies have been removed is residually *n*-type, this interface is a *p*-*n* junction. This model is similar to that proposed by Belas, *et. al.*. The junction depth is calculated as^{7,11}:

$$d = kGt/N_A A$$

where *k* = constant, dependent weakly on bombardment ion and its energy; *t* = time, *G* = number of ions striking

the HgCdTe per second, *N_A* = concentration of mercury vacancies initially present and *A* = bombardment area. Ion beam milling has been primarily used for type *p*-to-*n* conversion. Its application to device patterning has been rather limited or to the best of our knowledge; reported data on the topic is scarce. The authors report a few investigative studies pertaining to the technique on HgCdTe wafers and devices.

2.1.1 HgCdTe Wafers

Lunn¹² *et al.* examined the defect structure of *x* = 0.2, 0.21 HgCdTe after the sample was milled for 2 h with a current density of 600 μA/cm². The surface was free of dislocation tangles or individual dislocations and the microstructure consists of a uniform distribution of small dislocation loops¹². Their average diameter was approximately 40 nm and their density was approximately 10¹³ cm⁻² of foil area. No loops were observed in very thin areas of the foil close to the edge and observation of the extinction contours showed that the top 50 nm do not contain any loops. There is little change in the number of loops as the foil thickness increases above 50 nm and it is concluded that loops are confined to a fairly narrow band situated about 50 nm from the bombarded surface. Milling rate was observed to increase from 10 μm/h to 18 μm/h as ion current density increased¹² from 200 μA/cm² to 600 μA/cm². Milling rate is nonlinear with a tendency to saturate at higher beam current. Increase in current density will lead to a rise in the surface temperature that would lead to an increase in the milling rate^{11,12}. The milling rate saturates at higher current densities due to Hg loss and the associated compositional changes, causing a decrease in sputtering efficiency. Mittal,¹¹ *et al.* and Haakenaasen,¹³ *et al.* examined the variation of junction depth with milling time (Fig. 1). Junction depth increases with decrease in the vacancy concentration. Junction depth increases linearly with time and milling current density for depths up to 4 μm and then possibly as the square root of time at larger depth. For the same annealing temperature, high *x* samples have lower carrier concentration and greater junction depth than low *x* samples¹³.

2.1.2 HgCdTe MIS Devices

Bahir,¹⁴ *et al.* examined the effect of ion beam milling on carrier concentration and excess carrier lifetime of MIS devices¹⁴. Ion energy varies from 100 eV to 150 eV. They studied the effect of low temperature annealing (75 - 80 °C for 1 day to 1 week) following the milling process. They demonstrated that annealing reduces the carrier concentration slightly but has almost no effect on the carrier mobility or the induced depth profile. However, it affects the excess carrier lifetime. The lifetime for the as-grown material is of the order of microseconds, which is reduced to a few nanoseconds after milling. Annealing improves the lifetime to a few hundred nanoseconds after annealing. Figure 2 shows the temperature dependence of mobility and lifetime before and after ion beam milling, respectively.

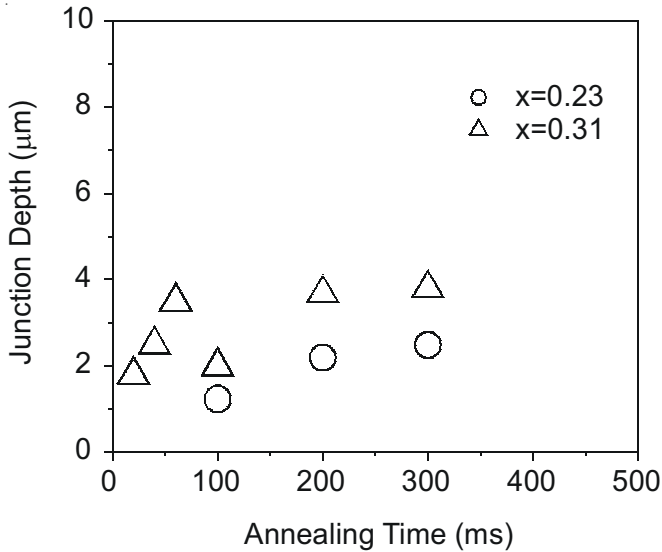


Figure 1. Junction depth vs annealing time at annealing temperature of 325 °C and ion current density of 0.14 mA/cm² for $x = 0.23$ and 0.31 ²¹.

Elkind carried out electrical measurements on MIS devices built on a wafer of *n-HgCdTe* ($x = 0.22$) measuring $2.1 \times 0.5 \times 0.08$ cm³. A 4 μm deep groove (250 μm wide) was ion milled into the wafer¹⁵. Ion mill damage, the severity of which was inversely proportional to the distance from the ion-milled stripe could be seen as far away as 150 μm. They also carried out the annealing of the same samples at 185 °C. A significant drop in lifetime between 12 h and 18 h was observed.

2.2 Ion Implantation

An alternative technique for making an *n* on *p* junction is implantation of an electrically inactive species into *HgCdTe* with a high concentration of a *p* type dopant (either mercury vacancies or an extrinsic acceptor on the cation sublattice)

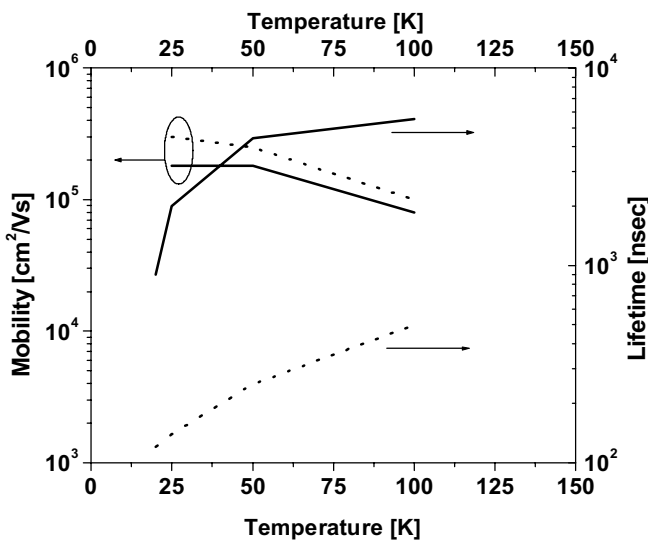


Figure 2. Temperature dependence of mobility and excess carrier lifetime before and after a 60-minute ion beam mill at energy of 100 to 110 V at ion current density of 0.5 mA/cm² for $x = 0.215$ *HgCdTe*¹³.

and a lower concentration donor¹⁶. Junction formation takes place irrespective of the valency of the bombarding ions^{17,18}. Elements such as *H*, *Hg*, *Al*, *Be*, *B* and *In* are used as implant species for making *n⁺-on-p* photodiodes. Out of these *B* is a favored implant species due to its small mass which minimises the crystal damage³. Ion implantation in MCT always results in *n⁺* whether the implanted impurity is donor acceptor or neutral and the electron density may be 10X of implanted dose- implying that damage is responsible. During ion implantation, *Hg* interstitials are generated mainly by two mechanisms. As the implanted ion collides with the lattice atoms in the sample, it loses some of its energy by creating Frenkel defects (interstitial vacancy pairs)¹⁶. The interstitials generated may also create further Frenkel defects, propagating a ‘collision-cascade’. Most of the Frenkel defects will recombine with one another during the collision cascade itself. A few point defects will survive however, if the recoil becomes physically displaced from its original position. This can occur if the energy transferred to recoil is large and/or if the recoiled atom is knocked into a crystal channel.

Regions of excess vacancies and interstitials are created when the distance separating them is too great for recombination to occur. *Hg* interstitials can also be created during implantation from the exchange of an implanted ion with a substitution *Hg* atom. If the concentration of excess interstitials exceeds the threshold value for extended defect formation, the excess interstitials will coalesce into dislocations or other types of extended defects. Following the implant, *HgCdTe* is annealed at a low temperature. During anneal, the *Hg* interstitials are released from the damage region and diffuse into the bulk *HgCdTe*^{17,18,19}. The interstitials annihilate *Hg* vacancies and/or exchange places with dopants on the cation sublattice, creating mobile dopant interstitials. When the concentration of acceptors is below that of donors, the region is converted to *n* type. The junction depth and shape are determined by the dose of trapped interstitials, the rate at which the interstitials are released from the damage region, the concentration of vacancies and extrinsic acceptors, and the rates at which the interstitials and dopants interact. Junction depths as a function of implant and anneal condition can be predicted when these parameters are known. The junction depth depends upon

- (a) implantation energy and dose,
- (b) thickness and type of cap layer,
- (c) substrate concentration including the background concentration and
- (d) annealing schedule.

In Figures 3 and 4, the authors have compiled the data available in literature and shown the variation of R_0A product as a function of composition x at different ion energies and ion doses, respectively⁴.

It may be seen from these figures that

The dose of *B⁺* ions is largely in the range of 1×10^{13} - 1.0×10^{14} , and the energy of *B⁺* ions mostly lies in the range of 100 keV-250 keV.

Most workers have used single implants.

The ion dose and energy are not the only criteria to

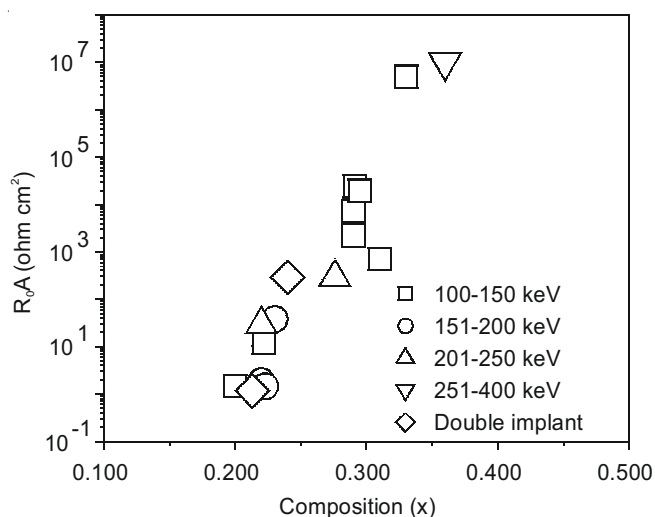


Figure 3. Composition dependence of R_0A as a function of implanted ion energy⁴ and references therein.

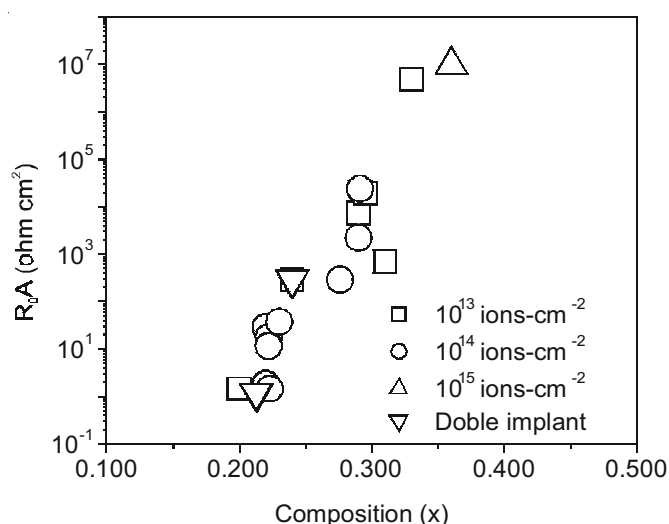


Figure 4. Composition dependence of R_0A as a function of implanted ion dose⁴ and references therein.

determine R_0A product, but the material properties are crucial.

Ion implantation introduces a controlled amount of damage and it is compatible with standard masking techniques used in semiconductor microelectronics. It allows the accurate control of the junction area with very small lateral extension leading to the possibility of achieving very small geometry diodes.

3. FABRICATION OF HDVIP'S AND AVALANCHE PHOTODIODES

Avalanche photodiode detector geometry is based on HDVIP architecture, which employs ion etch/mill to form loopholes in the device. The HDVIP device is designed as a cylindrical n - on- p or $n^+/n^-/p$ photodiode that is formed around a small via in $HgCdTe$ ^{25,26}. Via is etched through $HgCdTe$ by ion milling or implantation and serves as an interconnect conduit between n -side of the junction

and input to the Si- readout circuit. The HDVIP architecture is currently employed for large LWIR and MWIR staring arrays production at DRS Infrared Technologies²⁵⁻²⁷. APD operation in $HgCdTe$ spans a broad range of composition from $x=0.7$ to $x=0.2$ ²⁵. The fabrication process starts with a group-II site vacancy doped p -type $HgCdTe$ membrane (6-9 μm thick, $2-5 \times 10^{16} \text{ cm}^{-3}$). Group IB impurities are introduced to reduce diode spreading during ion milling. The wafer is counterdoped with donor In ($\sim 2 \times 10^{14} \text{ cm}^{-3}$) and a $CdTe$ passivation layer is deposited on front and back side of the membrane. Via is then etched using an Ar ion etch; the process creates a flux of Hg interstitials that fills metal vacancies and pushes out group IB acceptor impurities. The result is an n^- region doped in 10^{14} range by the residual In donor. The etch damage at the surface of the via results in a thin n^+ layer, thus forming a cylindrical $n^+/n^-/p$ diode. Initially RIE systems were used to etch deep vias in $HgCdTe$, but chemical nature of the etch results in a undesirable Cd rich layer around the via and also put limits on least via diameter that can be etched. For improving fill factor of the diodes, via diameter should be small for a fixed pitch to increase the optically active area²⁵. Purely physical nature of ion beam etch helped in circumventing these problems and proved more suitable for production of very high-density III-generation APD's. Kinch^{25,26} *et al* have reported fabrication of MWIR APD's ($\lambda_c = 5.2, 4.3 \mu\text{m}$, pitch = 40 μm and via dia = 6 μm), with gains greater than 100 at very low noise levels^{25,26}. Similar experimental work is being carried out at DRS technologies to fabricate HDVIP detectors with visible and near-IR (VNIR) response ($\lambda_c = 2.5 \mu\text{m}$)²⁷. The devices had quantum efficiency of 0.7–0.9 in the visible region with a high gain and desired responsivity.

4. DEMERITS OF DRY PROCESS METHODS

Ion bombardment during dry processing can lead to several undesirable changes in the electrical and optical properties of the soft and damage prone $HgCdTe$ substrate. Some of these aspects are discussed here with reference to the data collected from different sources.

4.1 Electrical Properties

Both ion milling and RIE systems operate at pressures of 100–400 mTorr with ion energies >100 eV. These systems induce type conversion and damages in the processed devices, particularly p -type material¹. Ion milling of $HgCdTe$ results in creation of extensive structural defects, type conversion of p -type $HgCdTe$ extending to large distances ($\sim 200 \mu\text{m}$) for short process times and produces long-range isotropic damage in n -type $HgCdTe$ ²⁸⁻³⁰. Smith, *et al.* performed a study of the spatial changes in electrical characteristics of $HgCdTe$ photoconductive (n -type) and photovoltaic (p -type) fabricated by RIE system³¹. A comparison between minority carrier lifetimes of wet processed device (10.5 μs) and RIE processed device (3.7 μs) showed a decrease by a factor of three in case of the dry processed device. This in turn results in decrease in responsivity, which has been interpreted as a loss of photo-generated

carriers. Reduction in performance can be attributed to mesa sidewall damage, lateral n+ doping and/or the introduction of additional re-combination mechanisms.

4.2 Co-lateral Damages/Surface Effects

Ion beam processing results in preferential etching of HgTe at the HgCdTe surface, leaving behind a Cd rich damaged layer and excess Hg on the surface³⁰. Surface damage propagates deep inside HgCdTe with a long tail and with lateral conversion³⁰. Exposures to plasma were found to result in surface roughening of HgCdTe. HDP etching of HgCdTe using low energy Ar ion bombardment has a sputter component at high DC bias values and results in increased Hg removal³². The damage depth due to sputtering has been estimated to be <10 nm at operating bias voltage³³. The properties of sidewall of the mesa may be different and are difficult to characterise.

However dry processing, particularly HDP etching is capable of reducing the pixel pitch and dramatically improving fill factors needed for high-density detector arrays. Hence for a given unit cell design parameters (etch depth, width, mesa profile and process time), the dry etch process has to be optimised to give high performance diodes.

5. CONCLUSION

The paper covers important aspects, salient features and technical challenges associated with various dry processes used in the fabrication of HgCdTe devices. Ion implantation and ion milling from the device as well as process perspective are accounted for. Ion irradiation creates damage sites in HgCdTe causing type conversion. This comes with a pressing need to eliminate dry etch damage. HDPE technologies result in low material damage. On the whole, dry processes combine high anisotropy, faster etch rates and better dimensional control.

REFERENCES

1. Srivastav, V.; Pal, R. & Vyas, H. P. Etching of mesa structures in HgCdTe, *OptoElectronics Review*. 2005, **13**(3), 197-211.
2. Smith, E. P. G.; Musca, C. A.; Redfern, D. A.; Dell, J. M. & Faraone, L. Reactive Ion Etching for Mesa Structuring in HgCdTe, *J. Vac. Sci. Technol.* 1999, **A17**(5), 2503-509
3. Agnihotri, O. P.; Lee, H. C. & Yang, Keedong. Plasma induced type conversion in mercury cadmium telluride, *Semicond. Sci. Technol.* 2002, **17**(10), R11-19
4. Altaf, E.; Pal, R.; Srivastav, V.; Gupta, S.; Dhar, V. & Vyas, H.P. Dry Processes for HgCdTe Infrared Detector Arrays, *Invertis J.. Sci & Technol.*, 2007, **1**(4), 260-79.
5. Engineering Thin Films and Nanostructures with Ion Beams, Ed. Emile Knystautas, CRC Press, 2005, p.9-11.
6. Wotherspoon, J.T.M. Method of manufacturing a detector device, UK Patent GB2095898, 1981
7. Blackman, M.V.; Charlton, D.E.; Jenner, M.D.; Purdy, D.R.; Wotherspoon, J.T.M.; Elliot, T.C. & White, A.M. Type conversion in Cd_xHg_{1-x}Te by ion beam treatment, *Electronics Letters*, 1987, **23**, 978 -79.
8. Baker, I. M. & Ballingal, R. A. Photovoltaic CdHgTe-silicon hybrid focal planes, *SPIE Proceedings*. 1984, **510**, 121.
9. Baker, I. M.; Jenner, M. D.; Parsons, J.; Ballingal, R. A.; Blenkinsop, I. D. & Firkins, J. H. Two dimensional random access infrared arrays, *IEE Conf. Publ.* 1983, **228**, 12.
10. Bleas, E.; Hoschl, P.; Grill, R. ; Franc, J.; Moravec, P.; Lischka, K.; Sitter, H. Type conversion of p-(HgCd)Te using H₂/CH₄ and Ar reactive ion etching, *J. Crystal Growth.*, 1994, **138**, 940-43.
11. Mittal, Vandna.; Gupta, Indu.; Sharma, R.K.; Singh, R.; Arora, S.C.; Singh, K.P.; Singh, B.V.; Gopal, V.; Kumar, V.& Basu, P.K. Study of Ion Beam Milling Effect on Some Electrical Properties of HgCdTe, Proceedings of the Eleventh International Workshop on the Physics of Semiconductor Devices, Eds. 2001, 1125-128.
12. Lunn, M.A. & Dobson, P.S. Ion beam milling of Cd_{0.2}Hg_{0.8}Te, *J. Cryst. Growth*. 1985, **73**, 379 -84
13. Haakenaasen, R.; Colin, T.; Steen, H. & Trodahl, Iversen, L. Planar n-on-p ion milled mid-wavelength and long-wavelength infrared diodes on molecular beam epitaxy vacancy-doped CdHgTe on CdZnTe, *J. Electron. Materials*. 2000, **29**(6) 849 -52.
14. Bahir, G.& Finkman, E. Ion beam milling effect on electrical properties of HgCdTe, *J. Vac. Sci. Technol.* 1989, **A7**(2), 348-353.
15. Elkind, J.L. Ion mill damage in n-HgCdTe, *J. Vac. Sci. Technol.* 1992, **B10**(4) 1460-465.
16. Holander-Gleixner, S.; Williams, B.L.; Robinson, H.G. & Helms, C.R. Modelling of junction formation and drive-in in ion implanted HgCdTe, *J. Electron. Mat.* 1997, **26**, 629-34.
17. Kolodny, A. & Kidron, I. n-channel MOS transistors in mercury cadmium telluride, *IEEE Trans. Electron. Devices*. 1980, **ED-27**, 37-43.
18. Bubulac, L.O. Ion implantation and diffusion for electrical junction formation in CdHgTe, *SPIE Proceedings*, 1991, **1484**, 67-71
19. Igras, E.; Piotrowski, J.& Zimnoch-Higersberger, I. Investigation of Ion Implanted Graded Gap (CdHgTe) Photodiodes, *Electron Technol.* 1977, **10**, 63.
20. Conway, K.L.; Opyd, W.G.; Greiner, M.E.; Gibbons, J.F.; Sigmon, T.W. & Bubulac, L.O. Thermal pulse annealing of boron implanted HgCdTe. *Appl. Phys. Lett.* 1982, **41**(8) 750-52.
21. Baars, J.; Flurrie, A.; Rothemund, W.; Fritzsche, C. R. & Jakobus, T. Boron ion implantation in Hg_{1-x}Cd_xTe, *J. Appl. Phys.* 1982, **53**(3), 1460-466.
22. Bubulac, L. O.; Lo, D. S.; Tennant, W. E.; Edwall, D. D.; Chen, J. C.; Ratusnik, J.; Robinson, J. C. & Bostrup, G. Ion implantation junction formation in Hg_{1-x}Cd_xTe, *J. Appl. Phys.* 1987, **50**(2) 1586-588.

23. Kumar, R.; Dutt, M. B.; Nath, R.; Chandra, R. & Gupta, S.C. Boron ion implantation in p-type $\text{Hg}_{0.8}\text{Cd}_{0.2}\text{Te}$, *J. Appl. Phys.* 1990, **68**(11), 5564-588.
24. Destefanis, G. L. Indium ion implantaion in $\text{Hg}_{0.78}\text{Cd}_{0.22}\text{Te}/\text{CdTe}$, *J. Vac. Sci. Technol.* 1985, **A 3**(1), 171-75
25. Beck Jeffrey, D.; Wan Chang, Feng.& Kinch Michael, A. MWIR *HgCdTe* avalanche photodiodes, *SPIE Proceedings*, 2001, **4454**.
26. Kinch, M..A.; Chandra, D.; Schaake, H.F.; Shih, H.D. & Aqariden, F. Arsenic doped mid-wavelength infrared *HgCdTe* photodiodes, *J. Electron. Mater.* 2004, **33**, 590-95.
27. Stapelbroek, M. G. ; Guptill, M.; D'souza, A.I.; Bryan, E.; Beck, J.; Kinch, M. & Robinson. Visible response of $\lambda=2.5$ m *HgCdTe* HDVIP detectors *SPIE Proceedings*. 2004, **5406**, 31-37.
28. Belas, E.; Hoschl, P.; Grill, R.; Franc, J.; Moravec, Lischka, & Sitter. Ultrafast diffusion of Hg in $\text{Hg}_{1-x}\text{Cd}_x\text{Te}$ *J. Cryst. Growth*, 1994, **138**, 940-53.
29. Smith, E.P.G.; Venzo, G.M ; Goetz, P.M.; Varesi, J.B.; Pham, L.T.; Patten, E.A.; Radford, W.A.; Johnson, S.M.; Stoltz, A.J.; Bensen, J.D. & Dinan, J.H. Inductively coupled plasma etching of *HgCdTe*, *J. Electron. Mater.* 2003, **32**, 821-26.
30. Pal, R. ; Chaudhury, P. K.; Sharma, B. L.; Kumar, V.; Musca, C. A.; Dell, J. M. & Faraone, L. Uniformity in *HgCdTe* Diode Arrays Fabricated by Reactive Ion Etching, *J. Electron. Mater.* 2004, **33**.
31. Smith, E.P.G.; Musca, C.A.; Redfern, D.A.; Dell, J. M. & Faraone, L. H_2 -based dry plasma etching for mesa structuring *HgCdTe* *J. Electron. Mater.* 2000, **29**, 853.
32. Eddy, Jr. C.R.; Shamamian, L.V.A.; Meyer, J.R.; Hoffman, C.A. & Butler, J.E. Characterization of the $\text{CH}_4/\text{H}_2/\text{Ar}$ high density plasma etching process for *HgCdTe* *J. Electron. Mater.* 1999, **28**, 347-52.
33. Stoltz, A.J. & Benson, J.D. The effect of electron cyclotron resonance parameters on the aspect ratio of trenches in *HgCdTe*, *J. Electron. Mater.* 2002, **32**, 692-97.